

IV. Ferroelectrics and Other Ferroic Materials

Dielectric polarization can be traced to several atomic mechanisms [1]. When an electric field is applied to a solid, electric charge is displaced, creating polarization. The field-induced dipole moment p is proportional to the local electric field, E_{loc} :

$$p = \alpha E_{loc}.$$

The total polarizability α can be written as the sum of four terms representing the most important contributions to the polarization.

$$\alpha = \alpha_e + \alpha_i + \alpha_d + \alpha_s.$$

Electronic polarizability α_e is caused by the displacement of the atomic electron cloud relative to the nucleus. As shown in Fig. 30, the negatively-charged electrons move antiparallel to the field creating an electric dipole parallel to the field. Electronic polarizability contributes to polarization in all solids, since all are made up of atoms. It is the chief contributor in materials such as diamond in which ionic and dipolar effects are absent.

Ionic polarizability α_i arises from the relative movements of positive and negative ions. Cations are displaced parallel to the local field, and anions in the opposite direction. As might be expected, such effects are most important in alkali halides and other ionic solids.

Some molecular solids contain permanent electric dipoles. In an electric field, the dipoles may change orientation. A number of hydrogen-bonded solids exhibit *dipolar polarizability* α_d , a strongly temperature-dependent effect in which protons switch sites.

Space charge polarizability α_s comes from migrating charge carriers in the dielectric. Migratory cations collect near the cathode and anions near the anode, distorting the electric field and increasing the capacitance of the solid. Good ionic conductors show pronounced space charge effects. Impurities sometimes make an important contribution to α_s .

The four types of polarizability display different frequency dependence. All four contribute to low-frequency polarization, but space charge currents are unable to follow radio-frequency fields in most insulators.

1. Polar Crystals and Pyroelectricity

79

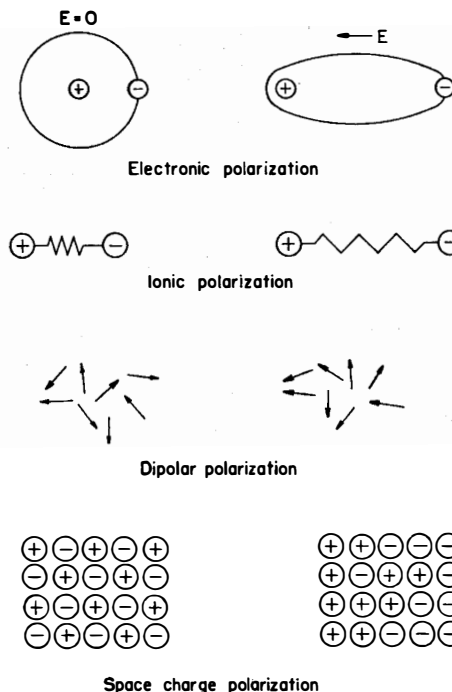


Fig. 30. Atomic contributions to electric polarization [1]

The dipolar contribution drops out in microwave region where rotational resonance and relaxation spectra occur. Ionic polarizability disappears in the infrared range, while the electronic portion continues through the visible to the near ultraviolet. The dielectric constant decreases with increasing frequency, approaching unity in the ultraviolet and X-ray region.

1. Polar Crystals and Pyroelectricity

Pyroelectric crystals contain a unique polar axis — a vector direction unrelated by symmetry to any other direction, not even the antiparallel direction. Such crystals contain a “built-in” spontaneous polarization P_s . In general, P_s changes with temperature, giving rise to a pyroelectric coefficient π defined by $\Delta P_s = \pi \Delta T$. The pyroelectric effect has been utilized in infrared detectors.

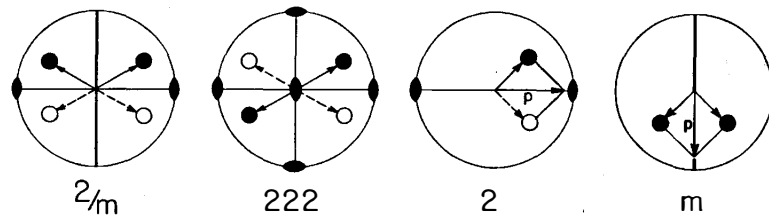


Fig. 31. Dipole configurations in two monoclinic and two orthorhombic point groups. In centric point groups like $2/m$, every dipole is cancelled by an equal and opposite dipole. These point groups are neither pyroelectric nor piezoelectric. Dipole cancellation also occurs in certain acentric point groups such as 222 . These point groups are generally piezoelectric but not pyroelectric. Dipoles do not cancel in point groups 2 and m which are both piezoelectric and pyroelectric. In 2 , the net spontaneous polarization must lie along the rotation axis. In m , P_s lies somewhere in the mirror plane

The symmetry restrictions on pyroelectricity can be visualized from stereographic diagrams of the crystallographic point groups (Fig. 31). Take a general point and operate on it with the symmetry elements of the group, generating a complete set of equivalent points. Connect the origin to each point, giving a set of vectors representative of the dipole configuration. The sum of these vectors gives the macroscopic polarization. Of the thirty-two point groups, non-zero polarizations are obtained for only ten, the ten pyroelectric point groups with a unique polar axis. In all but two classes (1 and m) the macroscopic polarization vector is oriented parallel to a rotation axis. The rotation axis is chosen along c in $6mm$, $4mm$, 4 , $3m$, 3 and $mm2$, and along b in monoclinic point group 2 .

Perhaps the simplest pyroelectric crystal is wurtzite, hexagonal ZnS (Fig. 32). The crystal class is $6mm$, for which the polar axis and P_s are parallel to c , the six-fold symmetry axis. The sign and magnitude of the spontaneous polarization in wurtzite can be estimated from the structure [2]. The wurtzite structure can be visualized as alternating layers of positive (zinc) and negative (sulfur) ions with equal numbers in each layer stacked perpendicular to c . Since each layer contains all positive ions or all negative ions, the polar chains in Figs. 32b and 32c can be used to calculate P_s . In computing P_s , a neutral portion of the crystal is chosen and p , the dipole moment per molecule, is calculated from $p = 1/n \sum_i q_i r_i$. Here n is the number of molecules, and q_i and r_i are the charge and position vector for the i th ion, respectively. The choice of origin is unimportant for a neutral collection of charges ($\sum_i q_i = 0$), but p does depend on the crystal boundary. If the specimen is terminated as in Fig. 32b, as would seem most likely, $p = +q(1/2 - u)c$. The termination

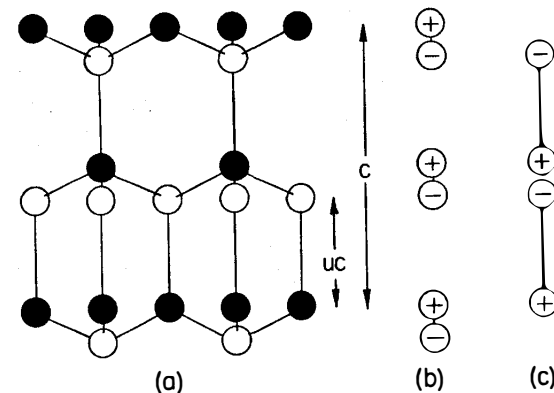


Fig. 32a-c. Wurtzite structure projected on (010), and equivalent polar chains showing two ways in which the crystal can terminate

in Fig. 32c leads to $p = -quc$, where the positional parameter u is $3/8$ for regular tetrahedra. Thus, the nature of the surface layer is important in relating spontaneous polarization to structure. Configuration (c) seems less likely than (b) because each surface atom is joined to the crystal by three bonds in (b) but only by one in (c).

The spontaneous polarization is related to the dipole moment per molecule by $P_s = Np$, N being the number of molecules per unit volume. Since there are two molecules in a cell of volume $\sqrt{3}a^2c/2$, the spontaneous polarization is $P_s = 4q(1/2 - u)/\sqrt{3}a^2$, assuming the termination in Fig. 32b is correct. P_s is difficult to measure directly but the change in P_s with temperature, the pyroelectric effect, has been measured for a number of polar crystals. For wurtzite, the pyroelectric coefficient π will depend on how q , u , and the lattice parameter change with T . It has been found that thermal expansion accounts for most of the pyroelectric polarization in tourmaline and rochelle salt.

Pyroelectric crystals are used as infrared radiation detectors. A pure capacitance type pyroelectric detector does not show Johnson noise so that the sensitivity is generally limited only by amplifier noise. The detectors are capable of very high frequency response and can be made spectrally selective by using absorptive coatings on the upper electrode.

The ratio of the pyroelectric coefficient to the dielectric constant can be considered a figure of merit for a detector material. Table 10 shows that triglycine sulfate (TGS) has the highest figure of merit. The high permittivity of most oxide ferroelectrics is a disadvantage in detector applications.

Table 10. Comparison of pyroelectric detector materials [3]

Material	Operating temperature (°C)	Dielectric constant	Pyroelectric coefficient ($\times 10^{-7} \text{ C/}^\circ\text{C-cm}^2$)	Figure of merit ($\times 10^{-11}$)
Triglycine sulfate	40	35	1.3	300
Lithium sulfate	25	10.3	0.078	76
Rochelle salt	22	1000	0.2	2
Barium titanate	25	4100	0.6	1.5
Lead zirconate titanate	25	2200	0.6	3

2. Piezoelectricity

Certain crystals polarize under applied stress, giving a linear relation between polarization P and stress σ .

$$P_i = d_{ijk} \sigma_{jk}.$$

All piezoelectric coefficients d_{ijk} are zero in centric crystals and most simple inorganic compounds contain a center of symmetry. The twenty piezoelectric crystal classes are listed in Table 4. Quartz, sphalerite, and wurtzite are acentric, but contain other symmetry elements. Such materials develop polarization for some stresses but not for others. In quartz, for instance, a compressive stress along $[100]$ causes polarization, but a stress along $[001]$ does not. The model structure in Fig. 33 illustrates directional piezoelectric effects in a collection of point charges.

In some crystals the cause of pyro- and piezoelectricity can be readily identified. $\text{NiSO}_3 \cdot 6\text{H}_2\text{O}$ contains Ni^{2+} ions in octahedral coordination with six water molecules and pyramidal sulfite groups (Fig. 34). Tetra-valent sulfur, another lone-pair ion like Pb^{2+} , Bi^{3+} , and Sb^{3+} , is 0.6 \AA above the plane of the oxygen ions. In nickel sulfite hexahydrate, all the sulfite groups point in the same direction with the trigonal axis of the crystal coinciding with the symmetry axis of the molecule. It is easy to see why the crystal is piezoelectric when squeezed in this direction. Not all crystals containing pyramidal groups are piezoelectric, however. In $\text{Zn}(\text{BrO}_3)_2 \cdot 6\text{H}_2\text{O}$, neighboring BrO_3^- pyramids align in an antiparallel fashion, creating a center of symmetry in the crystal, though individual molecules are acentric.

Crystals containing tetrahedral groups are often piezoelectric; zincite, zincblende, quartz and tridymite are examples. The symmetry of a regular

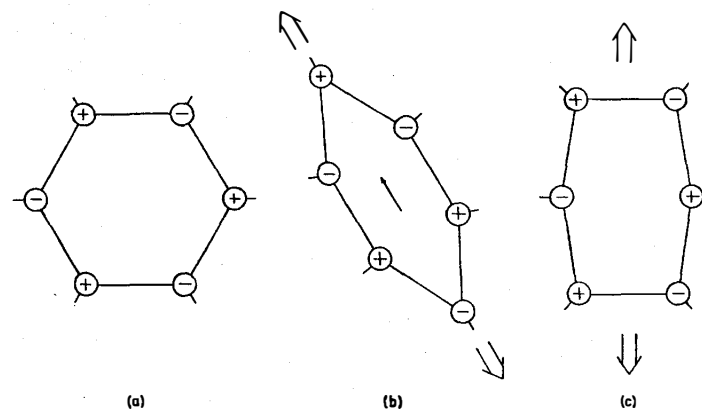


Fig. 33 a-c. Unstressed (a) and stressed (b, c) structures containing positive and negative ions. Polarization, a separation of positive and negative charge centers, is achieved in (b) but not in (c), showing that not all directions are piezoelectric

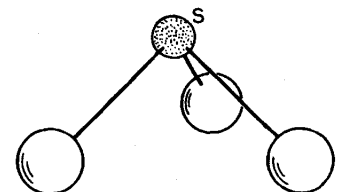


Fig. 34. The pyramidal sulfite group found in a number of piezoelectric crystals

tetrahedron is $\bar{4}3m$, a non-centrosymmetric point group. Crystals made up of acentric molecular groups have a greater probability of being piezoelectric than those containing centric groups.

Most piezoelectric crystals have rather complicated structures, but zincblende (cubic ZnS) is relatively simple. Zincblende belongs to crystal class $\bar{4}3m$ which has just one independent piezoelectric coefficient $P_1 = d_{14}\sigma_4$, in matrix notation. P_1 represents an electric polarization along $[100]$ and σ_4 is a shearing stress about $[100]$. JAFFE [4] has devised a theory showing how the sign and magnitude of the piezoelectric coefficient d_{14} is related to structure. When subjected to a shearing stress σ_4 , the crystal shears about x , changing the angle between y and z by an amount $\epsilon_4 = s_{44}\sigma_4$. The effect on a single tetrahedron in the zincblende structure is shown in Fig. 35. When sheared about a cube axis the two upper zinc atoms move closer to the sulfur, while the lower two move

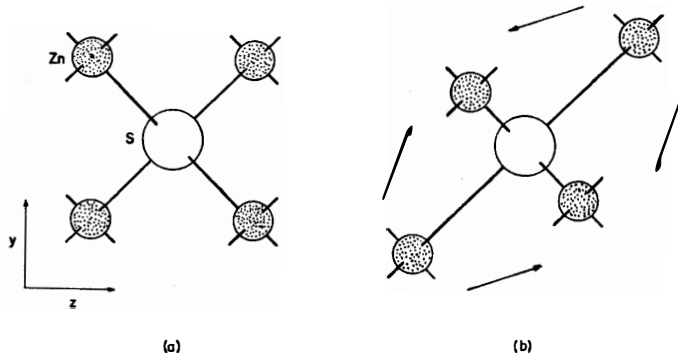


Fig. 35 a and b. A single tetrahedron of the zincblende structure, unstressed (a) and under shear stress (b), viewed along the polarization direction

further away. To maintain four equal bonds, the sulfur atom moves down in the $-x$ direction, toward the more distant zinc neighbors. From the geometry, the dipole moment per molecule developed along x is $-qa\epsilon_4/4$, where q is the charge of the sulfur ion and a is the cubic cell dimension. Since there are four molecules per cell, and all tetrahedra behave alike under the shearing stress, the resulting polarization is $P_1 = -qs_{44}\sigma_4/a^2$, giving $d_{14} = -qs_{44}/a^2$. Substituting experimental values for a , s_{44} , and d_{14} , JAFFE obtained $q = 0.25e$, a reasonable value for the charge, since the bonding in ZnS is largely covalent.

Piezoelectric quartz crystals are widely used as filters in telephone circuits and as frequency-control standards for radio oscillators. The resonant frequency of a thickness shear mode is

$$f = \frac{1}{2t} \sqrt{\frac{c}{\rho}},$$

where t is the thickness of the crystal plate, ρ is the density, and c the shear stiffness coefficient, which depends on orientation. In many applications it is necessary to control the frequency to within a few parts per million. Variations in ambient temperature result in unacceptable frequency drift unless the crystals are oriented properly. The variation in frequency with temperature is

$$\begin{aligned} \frac{1}{f} \frac{df}{dT} &= \frac{1}{2c} \frac{\partial c}{\partial T} - \frac{1}{t} \frac{\partial t}{\partial T} - \frac{1}{2\rho} \frac{\partial \rho}{\partial T} \\ &= \frac{1}{2c} \frac{\partial c}{\partial T} - \alpha_t + \frac{1}{2}(\alpha_1 + \alpha_2 + \alpha_3). \end{aligned}$$

The thermal expansion coefficient, α_t , is measured along the thickness direction. The thermal expansion coefficients, α_1 , α_2 , and α_3 , are measured along the principal axes. The elastic stiffness c , its temperature derivative $\partial c/\partial T$, and α_t all depend on crystal orientation. To prevent frequency drift with temperature, the crystal orientation is chosen in such a way that $df/dT = 0$. This is the principle behind the widely-used AT and BT quartz oscillator plates.

Temperature compensation is not possible in most piezoelectric crystals because dc/dT is generally negative and much larger than the thermal expansion term. Stiffness usually decreases with temperature as the bonding grows weaker. Only in exceptional cases do certain stiffness coefficients increase with temperature. The unusual behavior of the c_{66} coefficient of quartz is related to the α - β transition which involves rotational motions about the c -axis.

3. Acoustoelectric Effect

ZnO, CdS, GaAs, and other II-VI and III-V compounds crystallize in the wurtzite or sphalerite structures, which are acentric. Piezoelectric semi-conductor devices made from these materials amplify ultrasonic waves [5], employing the principle shown in Fig. 36. The acoustic wave generated by the transducer produces local mechanical strain, regions of compression and extension, which in turn produce electric fields through the converse piezoelectric effect. The local electric field has the periodicity of the acoustic wave and moves through the semiconductor where it interacts with conduction electrons, causing bunching of the charge carriers. As the acoustic wave moves, the electrons are dragged along and meet resistance, dissipating energy as heat. To maintain their velocity, the electrons extract energy from the local electric field which attenuates the acoustic wave.

Amplification rather than attenuation may result if an electric field is simultaneously applied to the semiconductor (Fig. 36). The electric field supplies energy to the conduction electrons, and if the field is adjusted to give electron velocities somewhat greater than the acoustic velocity, energy is transferred to the acoustic wave.

Gains of 50 db at frequencies near 100 MHz have been achieved but the inefficiency of electrical-mechanical energy conversion at the transducer-semiconductor interface creates coupling problems. One promising solution is to fabricate the insulating transducer from the same crystal as the semiconductor. This can be done by changing the impurity content, making an integrated device.

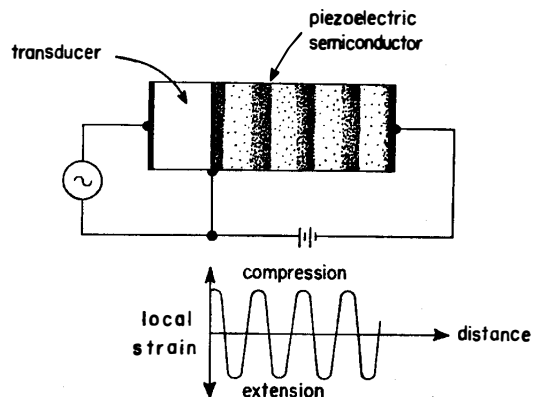


Fig. 36. Acoustoelectric experiment

4. Ferroelectricity

In some pyroelectric crystals the spontaneous polarization can be reversed by an applied electric field, giving a dielectric hysteresis loop. By analogy with ferromagnetism such crystals are called ferroelectric, even though iron is seldom a constituent. Ferroelectrics often exhibit large dielectric permittivities and piezoelectric coefficients. Ceramic capacitors of BaTiO_3 with dielectric constants in excess of 2000 are made commercially. Poled ceramics of $\text{Pb}(\text{Zr}, \text{Ti})\text{O}_3$, another perovskite-like ferroelectric, are widely used in sonar and other transducer applications.

Several hundred ferroelectrics have been reported since the discovery of the first ferroelectric fifty years ago. Among the oxide ferroelectrics, many are titanates, niobates and tantalates, crystallizing in the perovskite structure, or one of the related structures based on oxygen octahedra. The ground state electron configurations of Ti, Nb, and Ta involve competing d and s electrons of nearly equal energy which promote the asymmetrical bonding leading to ferroelectricity.

Another group of asymmetrical ions are those with "lone-pair" electron configurations. Pb^{2+} , Bi^{3+} , Sn^{2+} , Te^{4+} , I^{5+} , Sn^{3+} and several other ions have two electrons outside a closed d shell. The two outer electrons form a lone-pair orbital on one side of the ion, which promotes pyramidal bonding, as in NH_3 and the PbO structures. The pyramid has a dipole moment which results in spontaneous polarization when the dipoles do not cancel.

Ionic radii sometimes determine the types of distortions. Comparing compounds with the perovskite structure, ferroelectricity occurs in

BaTiO_3 and KNbO_3 , whereas nonpolar distortions are found in SrTiO_3 , NaNbO_3 , and CaTiO_3 . The radii of the cubo-octahedral ion appears to be crucial: the larger Ba^{2+} and K^+ ions promote polar motions, while the perovskite partially collapses around the smaller Sr^{2+} , Ca^{2+} , and Na^+ ions, producing antiparallel rotational motions.

Most ferroelectrics show a paraelectric-ferroelectric phase transition. In general, the symmetry of the ferroelectric form is a subgroup of the high-temperature (prototype) symmetry, but symmetry considerations do not dictate which of several derivative symmetries are most likely to occur. Atomistic energy arguments are needed to predict the most probable distortions.

Most inorganic materials are made up of basic building blocks such as the octahedra in perovskite-like materials. Such units tend to have strong internal bonding, resulting in short interatomic distances. Deformation of individual building blocks requires considerable energy because of the short-range repulsive forces between neighboring anions. Thus in predicting the derivative symmetry accompanying a phase transition, it is pertinent to examine the effect of a given symmetry change on the basic building blocks. Some symmetry changes require a change in shape of the basic unit, others do not and are therefore favored.

Structure analyses have shown that the oxygen octahedra in BaTiO_3 and PbTiO_3 remain fairly regular in the ferroelectric phase. In the bismuth titanate family—a group of ferroelectrics made up of perovskite layers separated by bismuth oxide layers—it is found that compounds with an odd number of perovskite layers crystallize in $B2_{cb}$, while even-layered members prefer $A2_{1am}$ [6]. The reason is strain energy: the observed symmetry changes enable oxygens to bond to the bismuth oxide layer without distorting the oxygen octahedra of the perovskite layer. Distortions of the octahedra lead to short O—O distances which are energetically unfavorable.

Bismuth tungstate (Bi_2WO_6) and bismuth titanium niobate ($\text{Bi}_3\text{TiNbO}_9$) are representative members of the bismuth titanate family. Figure 37 shows why a one-layer compound such as Bi_2WO_6 prefers $B2_{cb}$ rather than $A2_{1am}$. The single perovskite layer of the prototype structure is shown in Fig. 37a. The prototype structure belongs to space group $I4/mmm$ and when viewed along a , as in Fig. 37, shows $2mm$ symmetry with 2-fold axes along a and mirror planes perpendicular to b and c . Below the transition temperature the apex oxygens form a single short bond with bismuth, displacing the apex oxygen in the b -direction. This movement automatically destroys the vertical mirror planes perpendicular to b . Figures 37b and c show the consequences of retaining the remaining two symmetry elements. Keeping the mirror plane perpendicular to c results in deformation of the octahedra, as shown in

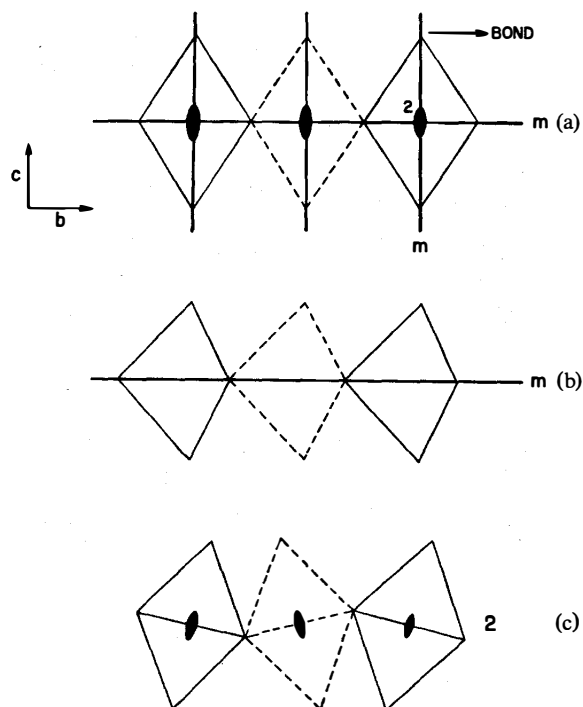


Fig. 37a-c. The perovskite sheet of Bi_2WO_6 viewed along a . When apex oxygens of the prototype structure (a) shift along b , the layer may retain mirror symmetry (b) or two-fold symmetry (c). The latter is energetically favorable because individual octahedra need not deform

Fig. 37b, but this is not so when the two-fold axes parallel to a are retained. In this case (Fig. 37c), the apices shift and the octahedra rotate without deforming. Thus B2cb which has a two-fold axis along a , is favored energetically over $\text{A2}_1\text{am}$, which retains a mirror perpendicular to c .

The reverse is true in $\text{Bi}_3\text{TiNbO}_9$ and other two-layer compounds because the symmetry elements of the prototype structure are positioned differently (Fig. 38a). The mirror plane perpendicular to c and the two-fold axes parallel to a intersect octahedral corners only. Vertical mirrors perpendicular to b are again destroyed when the outer apex oxygens bond to bismuth. Retaining mirrors perpendicular to c (Fig. 38b) allows the octahedra to rotate without deformation, which is not true on

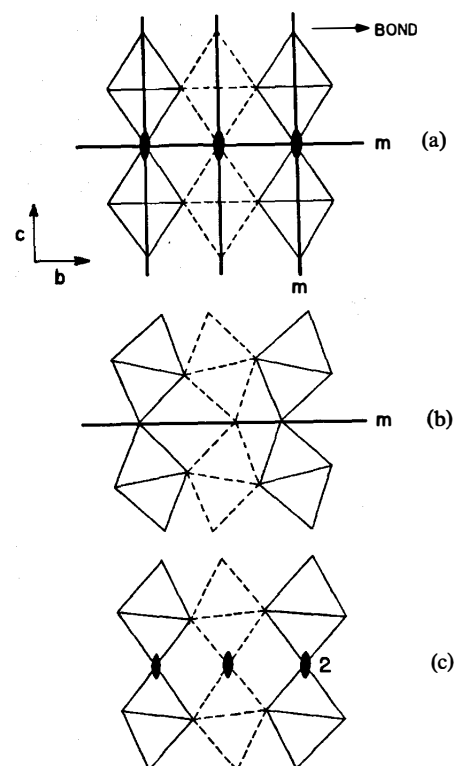


Fig. 38a-c. Symmetry elements of the double perovskite layer found in $\text{Bi}_3\text{TiNbO}_9$ are shown in (a). Shifting the apex oxygens parallel to b results in rotation of the octahedra, (b) and (c). Mirror symmetry does not require deformation of individual octahedra and is therefore favored

retention of the rotation axes (Fig. 38c). Strain is minimized in a two-layer perovskite by retaining mirror ($\text{A2}_1\text{am}$) rather than rotational (B2cb) symmetry.

5. Hydrogen-Bonded Ferroelectrics

Among other ferroelectrics, there are molecules and radicals which promote ferroelectricity. Rochelle salt is but one of many ferroelectric tartrates. Ferroelectrics are also common among sulfates, sulfites,

nitrates, and nitrites. None of the molecular groups in these crystals are centrosymmetric.

Hydrogen-bonding plays a key role in many ferroelectrics. The transition between the high-temperature paraelectric state and low-temperature ferroelectric state is essentially an order-disorder phenomenon. Above the transition, protons are statistically distributed among certain crystallographic positions. Long range ordering takes place below the transition, lowering the symmetry and causing ferroelectricity. The process differs from the ordering effect observed in CuAu in that diffusion is not required, and therefore the transition is displacive in character.

Potassium dihydrogen phosphate ($\text{KH}_2\text{PO}_4 = \text{KDP}$) and ammonium dihydrogen phosphate ($\text{NH}_4\text{H}_2\text{PO}_4 = \text{ADP}$) are good examples of a hydrogen bonded ferroelectric and antiferroelectric, respectively. The structures closely resemble zircon (ZrSiO_4), and consists of PO_4 phosphate groups bonded together by K^+ or NH_4^+ ions and hydrogen bonds. At room temperature the hydrogen atoms are disordered, occupying two sites with equal probability. Both structures undergo phase transitions at low temperatures, with the protons ordering in double potential wells.

In the room temperature structure of KH_2PO_4 , hydrogen ions are distributed statistically over two positions of equilibrium. The two sites are about 0.4 Å apart on the O-H-O bond. Below the Curie point, the hydrogens in KH_2PO_4 are in an ordered arrangement with two hydrogens near every PO_4 group. KH_2PO_4 polarizes along the c crystallographic axis with P_s either parallel or antiparallel to c , forming 180° domains. In domains with the spontaneous polarization parallel to c , the protons at the base of the tetrahedra move close and the upper ones move away (Fig. 39a). Applying an electric field parallel to $-c$ switches P_s and the lower protons move away while the upper protons move close. The hydrogen ions do not contribute to the spontaneous polarization since they move perpendicular to the ferroelectric axis. In so doing, however, the protons exert coulomb forces on the other atoms, causing the P^{5+} and K^+ ions to shift in the $+c$ direction, and oxygens along $-c$, producing the spontaneous polarization.

$\text{NH}_4\text{H}_2\text{PO}_4$ is nearly isomorphous with KH_2PO_4 but the proton ordering is different. The symmetry of KH_2PO_4 changes from $142d$ to $Fdd2$ at the transition, whereas the ammonium salt transforms from $142d$ to $P2_12_12_1$. At room temperature the acid hydrogens in $\text{NH}_4\text{H}_2\text{PO}_4$ are disordered, as in KH_2PO_4 , and at low temperatures they adopt the arrangement shown in Fig. 39. In this case, one lower H^+ and one upper H^+ move close to each PO_4 group, cancelling any shifts along c . Ammonium dihydrogen phosphate does not polarize spontaneously at

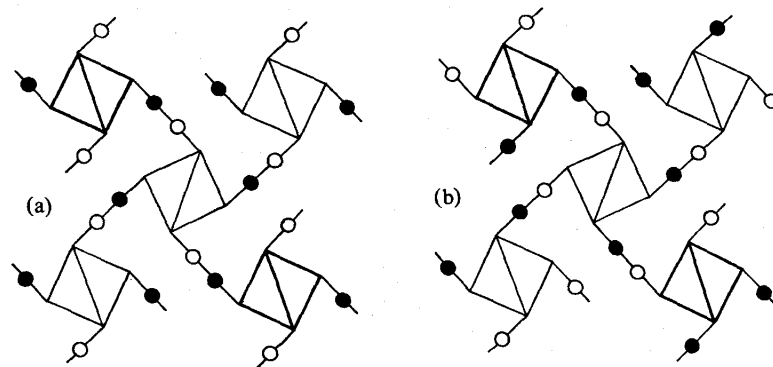


Fig. 39 a and b. Ordering of hydrogen ions on the O-H-O bonds in (a) ferroelectric KH_2PO_4 and (b) antiferroelectric $\text{NH}_4\text{H}_2\text{PO}_4$. Full and empty proton sites are represented by solid and open circles, respectively

the transition, and is, therefore, not a ferroelectric. It is called an antiferroelectric because of the antiparallel shifts, and because it is closely related to ferroelectric KH_2PO_4 .

6. Classification of Ferroelectrics

The dielectric constant κ of a ferroelectric reaches a maximum near the paraelectric-ferroelectric transition. Above the transition in the paraelectric state, the decrease in κ can be described by a Curie-Weiss Law. Perhaps the best empirical classification of ferroelectrics is by the Curie-Weiss constant C appearing in the Curie-Weiss equation

$$\kappa - \kappa_0 = \frac{C}{T - T_0}$$

κ is the dielectric constant, κ_0 the temperature-independent part, T the absolute temperature, and T_0 the extrapolated Curie temperature. It has been demonstrated [7] that the value of C is a better indication of the type of ferroelectric than is the transition temperature T_c , the extrapolated Curie temperature T_0 , or the transition entropy S .

There appear to be three important groups of ferroelectrics. In the BaTiO_3 type, C is about 10^5 and all have "active" ions tending to promote distortions. These are of two types: ions such as Ti^{4+} , Nb^{5+} , and W^{6+} in Columns IVB, VB, and VIB and "lone-pair" ions in Columns IVA and VA exemplified by Pb^{2+} , Bi^{3+} , and Sb^{3+} . Most of the

compounds in this family are oxides, with SbSI being a notable exception. Positive and negative ions undergo a displacive transition at the Curie temperature.

The second class is the order-disorder type with Curie-Weiss constants near 10^3 . Ordering of rotatable permanent dipoles takes place at the transition temperature. Such dipoles are associated with hydrogen bonds as in KH_2PO_4 , or with molecular groups such as the NO_2^- ions in sodium nitrite. Most of the water-soluble ferroelectrics are in this category.

The third group possesses small C values near 1, and are what have been termed improper ferroelectrics in which ferroelectricity results from piezoelectric coupling to an elastic instability. The best example of this class is the ferroelastic $\text{Gd}_3(\text{MoO}_4)_2$ —this is an active field of present day research and more good examples will appear.

Another classification scheme [8] is based on the dimensionality of the atomic displacements accompanying reversal. In a one-dimensional ferroelectric, atomic displacements are parallel to the polar axis. This class includes BaTiO_3 , PbTiO_3 , LiNbO_3 , SbSI and the tungsten bronze ferroelectrics, materials with large spontaneous polarizations ($\sim 25 \mu\text{C}/\text{cm}^2$) and relatively high symmetry. Atomic displacements in a two-dimensional ferroelectric lie in parallel planes containing the polar axis. All the known examples (BaCoF_4 , HCl , NaNO_2 , thiourea) crystallize in class $mm2$, and have medium-sized polarizations, around $5 \mu\text{C}/\text{cm}^2$. In many respects this class is intermediate between the ionic one-dimensional class and the three-dimensional class, the bulk of which are molecular. Three-dimensional ferroelectrics generally have complex structures, often with tetrahedral groups ($\beta\text{-Gd}_2(\text{MoO}_4)_3$), or with hydrogen bonds (guanidine aluminum sulfate hexahydrate), or both (KH_2PO_4). The group is characterized by low spontaneous polarizations, typically less than $3 \mu\text{C}/\text{cm}^2$. Polarizations tend to be small because atomic displacements perpendicular to the polar axis are compensated.

7. Transition-Temperature and Coercive Field

Control of the Curie point by chemical substitution is common practice in the electroceramics industry. Ferroelectric oxides are of interest as capacitor materials because of their high-permittivity levels, but the sharp maximum in dielectric constant at the Curie point must be broadened and moved to room temperature. The Curie point of BaTiO_3 is generally lowered and broadened when either Ba^{2+} or Ti^{4+} is partially replaced. Pb^{2+} is the only divalent cation which raises T_c , probably because of its high polarizability and aspherical electron

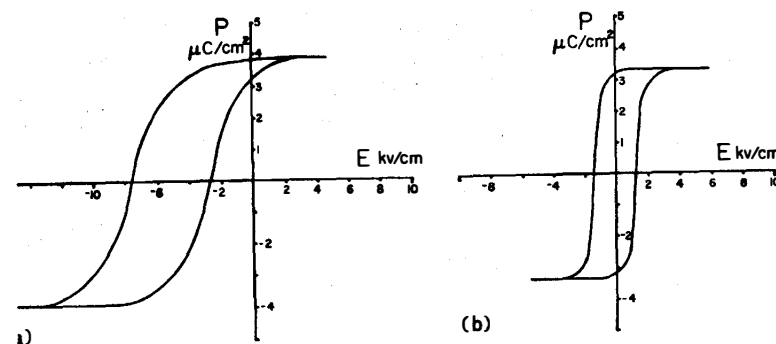


Fig. 40a and b. Ferroelectric hysteresis loops of (a) triglycine sulfate doped with L-alanine and (b) pure TGS

configuration. The shift caused by the lattice contraction accompanying the substitution of Sr for Ba corresponds quantitatively to the effect of hydrostatic pressure. T_c decreases much more rapidly when the active Ti^{4+} ion is replaced by Zr^{4+} , Sn^{4+} , or other tetravalent ions.

Permanent poling effects have been achieved in organic ferroelectrics by doping the crystals with low-symmetry organic molecules. Triglycine sulfate (TGS) is superior to most radiation detectors because of its high pyroelectric coefficient and low dielectric constant. Optimum efficiency is obtained in single domain crystals, hence accidental depoling must be avoided. TGS crystals grown from water solution containing several percent alanine show a permanent self-bias. Dielectric hysteresis loops (Fig. 40) are displaced along the field axis, a bias which is retained even after prolonged heating above the Curie point and after applying reverse-bias fields.

Alanine is sufficiently similar to glycine to substitute for it in TGS. The zwitter ion forms are illustrated in Fig. 41. The two molecules differ by a methyl group which imparts a handedness to the alanine molecule. Right-handed D-alanine (Fig. 41c) is the mirror image of L-alanine (Fig. 41b). When triglycine sulfate becomes polar, the glycine groups deform, adopting a handedness. During ferroelectric switching the molecule rotates and deforms, becoming its own mirror image. Replacing glycine with alanine biases the switching because of the irreversible handedness of the alanine molecule. Substituting only D-alanine (or only L-alanine) results in a poled single crystal useful for pyroelectric applications [9].

The key feature in substitutions of this type is violation of the prototypic symmetry. In transforming from the high temperature para-

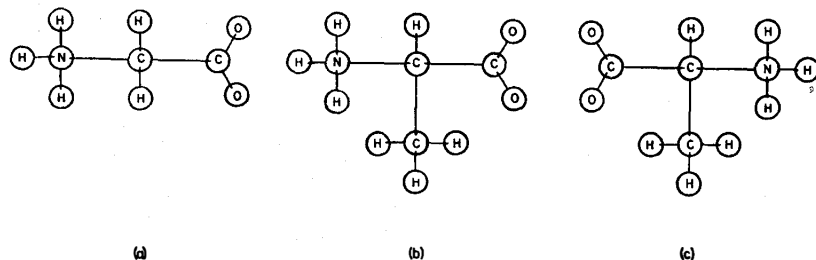


Fig. 41 a-c. Zwitter ion forms of (a) glycine, (b) L-alanine, and (c) D-alanine

electric state to the room-temperature ferroelectric modification, TGS loses mirror symmetry as it changes from monoclinic point group $2/m$ to 2. The alanine molecule does not possess mirror symmetry and on entering the TGS crystal destroys the prototypic symmetry. The technique can be applied to other ferroelectrics in which switching involves symmetry changes of certain atomic groups. Switching of this type can be impeded by substitution of a similar group which breaks the prototypic symmetry.

8. Ferroic Crystals

Ferroelectricity is but one example of a more general phenomenon in which a crystal can be switched between two orientation states by an applied force, or some combination of applied forces. AIZU [10] has developed a symmetry classification and terminology to describe the more general effects. Consider a composite crystal with two or more orientation states—a mimetically-twinned crystal. The structures of the individual domains may be identical (except for orientation), or they may be enantiomorphic.

In the past, twinned crystals have either been classified according to twin-laws and morphology, or according to their mode of origin, or according to a structural basis, but there is another classification scheme which deserves wider acceptance, one which is based on the tensor properties of the orientation states. An advantage of such a classification is the logical relation between free energy and twin structures, for it becomes immediately apparent which forces and fields will be effective in moving twin walls. The domain patterns in ferroelectric and ferromagnetic materials are strongly affected by external fields, but there are many other types of twinned crystals with movable twin walls and hysteresis. AIZU [10,11] has classified these materials as ferroelastic,

ferrobielectric, and various other ferroic species. As explained later, each type of switching arises from a particular term in the free energy function.

A *ferroic* crystal contains two or more possible orientation states or domains; under a suitably chosen driving force the domain walls move, switching the crystal from one domain state to another. Switching may be accomplished by mechanical stress (σ), electric field (E), magnetic field (H), or some combination of the three. Ferroelectric, ferroelastic and ferromagnetic materials are well known examples of primary ferroic crystals in which the orientation states differ in spontaneous polarization (P_s), spontaneous strain (ϵ_s) and spontaneous magnetization (M_s), respectively. It is not necessary, however, that the orientation states differ in the primary quantities (strain, polarization, or magnetization) for the appropriate field to develop a driving force between orientations. If, for example, the twinning rules between domains lead to a different orientation of the elastic compliance tensor, a suitably oriented stress can produce different strains in the two domains. The stress may act upon the difference in induced strain to produce wall motion and domain reorientation. AIZU [10] suggested the term ferrobielectric to distinguish this type of response, and illustrated the effect with Dauphine twinning in quartz. Other types of secondary ferroic crystals are listed in Table 11, along with the difference between domain

Table 11. Primary and secondary ferroics

Ferroic class	Orientation state differ in	Switching force	Example
Primary			
Ferroelectric	Spontaneous polarization	Electric field	BaTiO ₃
Ferroelastic	Spontaneous strain	Mechanical stress	CaAl ₂ Si ₂ O ₈
Ferromagnetic	Spontaneous magnetization	Magnetic field	Fe ₃ O ₄
Secondary			
Ferrobielectric	Dielectric susceptibility	Electric field	SrTiO ₃ (?)
Ferrobimagnetic	Magnetic susceptibility	Magnetic field	NiO
Ferrobielectric	Elastic compliance	Mechanical stress	SiO ₂
Ferroelastoelectric	Piezoelectric coefficients	Electric field and mechanical stress	NH ₄ Cl
Ferromagnetoelastic	Piezomagnetic coefficients	Magnetic field and mechanical stress	FeCO ₃
Ferromagnetoelctric	Magnetoelectric coefficients	Magnetic field and electric field	Cr ₂ O ₃

states, and the driving fields required to switch between states. The derivation of the various ferroic species from a free energy function is considered next.

9. Free Energy Formulation

The stability of an orientation state is governed by the free energy G . In differential form dG is comprised of thermal energy and various work terms

$$dG = SdT - \varepsilon_{ij}d\sigma_{ij} - P_idE_i - M_idH_i.$$

S is entropy, T temperature, ε_{ij} strain, σ_{ij} stress, P_i electric polarization, E_i electric field, M_i magnetization, and H_i magnetic field. The directional subscripts refer to cartesian coordinates; $i, j = 1, 2, 3$. The entropy term is neglected in what follows since we assume the experiments are performed under isothermal conditions.

Strain ε is measured relative to the prototype structure and can be written as a spontaneous strain $\varepsilon_{(s)}$ plus an induced strain. Induced strain may arise from applied mechanical stress (elasticity), from applied electric fields (piezoelectricity) or from applied magnetic fields (piezomagnetism).

$$\varepsilon_{ij} = \varepsilon_{(s)ij} + s_{ijkl}\sigma_{kl} + d_{kij}E_k + Q_{kij}H_k.$$

In this equation s_{ijkl} is a component of the fourth-rank elastic compliance tensor. The piezoelectric coefficients d_{kij} constitute a third rank tensor, as do the piezomagnetic coefficients Q_{kij} . Compliance and piezoelectricity are polar tensors whereas piezomagnetism is an axial tensor. Of the four terms in the expression for ε_{ij} given above, only the second term is always present. Piezoelectricity and piezomagnetism are null properties which disappear for certain symmetry groups, but all groups have non-zero elastic constants. Spontaneous strain is the change in shape measured relative to the prototype structure. Some twinned crystals possess spontaneous strain.

Electric polarization can be expanded in a manner similar to strain, with contributions from a spontaneous polarization $P_{(s)}$ and several induced effects.

$$P_i = P_{(s)i} + \kappa_{ij}E_j + d_{ijk}\sigma_{jk} + \alpha_{ij}H_j.$$

The second rank tensor κ_{ij} and α_{ij} represent the electric susceptibility and magnetoelectric coefficients, respectively. κ_{ij} is a polar tensor and α_{ij} is an axial tensor. Only the ten polar crystal classes possess

spontaneous polarization $P_{(s)}$. All materials have finite electric susceptibility coefficients, so that electrically-induced polarization is always present, but magnetoelectricity is found only in solids with certain types of magnetic symmetry.

Magnetization can be expanded in terms of the spontaneous magnetization, and induced effects arising from electric and magnetic fields, and mechanical stress.

$$M_i = M_{(s)i} + \chi_{ij}H_j + Q_{ijk}\sigma_{jk} + \alpha_{ij}E_j.$$

Only ferromagnetic and ferrimagnetic crystals have non-zero spontaneous magnetization. All materials possess non-zero magnetic susceptibility coefficients, (χ_{ij}) , but the induced magnetization is often very small.

Substituting the expression for ε_{ij} , P_i , and M_i into the differential form for free energy, combining terms, and integrating gives the thermodynamic potential G , which applies to all orientation states. Let 1G represent the free energy for the first orientation state and 2G for the second; with the tensor terms referred to a common axial system. The driving potential for a state shift is the $\Delta G = ^1G - ^2G$. In the absence of external fields and forces, the energy of all orientation states is equal, so that $\Delta G = 0$. Under external forces the difference in free energy for the two orientation states is

$$\begin{aligned} \Delta G = & \Delta\varepsilon_{(s)ij}\sigma_{ij} + \Delta P_{(s)i}E_i + \Delta M_{(s)i}H_i + \frac{1}{2}\Delta s_{ijkl}\sigma_{ij}\sigma_{kl} + \frac{1}{2}\Delta\kappa_{ij}E_iE_j \\ & + \frac{1}{2}\Delta\chi_{ij}H_iH_j + 2\Delta d_{ijk}E_i\sigma_{jk} + 2\Delta Q_{ijk}H_i\sigma_{jk} + 2\Delta\alpha_{ij}H_iE_j. \end{aligned}$$

$\Delta\varepsilon_{(s)ij}$ is $^2\varepsilon_{(s)ij} - ^1\varepsilon_{(s)ij}$, the difference in a certain component of spontaneous strain for orientation states 1 and 2. $\Delta P_{(s)i}$ and $\Delta M_{(s)i}$ are the differences in the i th component of spontaneous polarization and spontaneous magnetization for the two domains. Differences in elastic compliance coefficients are represented by Δs_{ijkl} . The remaining five terms in ΔG arise from differences in electric and magnetic susceptibility, and from differences in piezoelectric, piezomagnetic and magnetoelectric coefficients.

A wide variety of ferroic phenomena are possible, depending on which terms in ΔG are important. If $\Delta P_{(s)}$ is non-zero, the material is ferroelectric provided the coercive field does not exceed the electric breakdown limit. Materials with $\Delta\varepsilon_{(s)} \neq 0$ are ferroelastic if the mechanical stress required to switch orientation states does not result in rupture. Ferromagnetic domains—the third type of primary ferroic—possess finite differences in spontaneous magnetization.

The transition between domain states in a ferroelectric is said to be electrically first-order because ΔG is proportional to E . If $\Delta P_{(s)} = 0$ and $\Delta \kappa \neq 0$, then $\Delta G \sim E^2$ and the material is potentially ferroelectric. Other secondary ferroics are listed in Table 11. For a ferroelastic $\Delta G \sim \sigma^2$, and for a ferrobimagnetic $\Delta G \sim H^2$. Cross-coupled ferroics include the ferroelastoelectric ($\Delta G \sim E\sigma$), ferromagnetoelastic ($\Delta G \sim H\sigma$) and ferromagnetoelctric ($\Delta G \sim EH$).

Because of coupling coefficients, the classes are not mutually exclusive. For example, in any dielectric material there is a coupling between polarization and lattice strain through the piezoelectric or electrostrictive coefficients; if a crystal spontaneously polarizes, it also spontaneously strains. If all the orientation states of a ferroelectric differ also in the orientation of the strain tensor, then the material may be termed fully ferroelectric-fully ferroelastic. In most ferroelectrics, however, some but not *all* domain states differ in the orientation of the elastic strain tensor. For example in BaTiO_3 , 90° domains differ in the orientation of the strain tensor, but 180° domains do not. Such systems may be described as fully ferroelectric, partially ferroelastic. Cobalt ferrite is fully ferrimagnetic, partially ferroelastic, while nickel iodine boracite is fully ferroelectric, fully ferromagnetic and fully ferroelastic. In this type of material all domains can be reoriented by electric, magnetic or mechanical stress fields.

10. Primary Ferroic Minerals

Twinning is widely used in mineral identification and in elucidating the formation conditions of rocks. The distribution of transformation twins in rock-forming minerals enables one to establish the thermal processes that have occurred in the rock. Mechanical twinning is studied by petrologists in the analysis of flow effects. In rock magnetism, it is the arrangement of ferromagnetic domains which determines remanent magnetization. These are but a few examples of twin phenomena in minerals.

Ferroelectrics are fairly rare in the mineral kingdom. A *ferroelectric* is a crystal possessing reversible polarization, as shown by a dielectric hysteresis loop. Domains in a ferroelectric differ in spontaneous polarization $P_{(s)}$, and can be switched by an applied electric field.

A large number of ferroelectric compounds occur in the perovskite and pyrochlore families, although the minerals CaTiO_3 and $\text{CaNaNb}_2\text{O}_6\text{F}$ are not ferroelectric. Barium titanate and PZT (lead zirconate-titanate) are of considerable commercial importance because of their high permittivities and large piezoelectric coefficients. Other

mineral-related ferroelectrics are found in the boracite family and among nitrates such as KNO_3 -Phase III. However, the only ferroelectric investigated extensively using mineral specimens is colemanite, $\text{CaB}_3\text{O}_4(\text{OH})_3 \cdot \text{H}_2\text{O}$.

Ferroelectricity was discovered in the borate mineral colemanite by GOLDSMITH [12]. At room temperature colemanite is centric, point group $2/m$, but below approximately 0°C it transforms to a ferroelectric phase belonging to point group 2. Spontaneous polarization develops along the monoclinic b axis, accompanied by the formation of 180° domains. At -20°C the spontaneous polarization $P_{(s)}$ is $0.45 \mu\text{C}/\text{cm}^2$, and the coercive field required to switch domains is about $2000 \text{ V}/\text{cm}$ [13]. With increasing temperature $P_{(s)}$ decreases continuously to zero, typical of a second order transition. The Curie point is strongly affected by space charge fields caused by impurities, but for most natural specimens it ranges from 0°C to -7°C .

Ferroelectric domains are sometimes visible in polarized light, but the 180° domains in colemanite cannot be distinguished in this way since the optical indicatrix is identical for both orientation states. There is a possibility that the difference in optical activity could be utilized, though this has yet to be demonstrated. The orientation states in colemanite are enantiomorphic, and potentially optically-active. Because of this, the 180° domains may be visible when viewed along an optic axis.

The structural basis of ferroelectricity in colemanite has been described by HAINSWORTH and PETCH [14]. Above the transition, in the nonpolar phase, one of the hydrogen atoms of the water molecule and the hydrogen of an adjacent hydroxyl group are in a state of dynamic disorder. As the temperature is lowered, the rate of reorientation decreases until the hydrogens settle into ordered noncentric positions in the ferroelectric phase. The ordering of hydrogen atoms is accompanied by small displacements of other atoms from the positions they occupy in the centric phase.

The orientation states of a *ferromagnet* differ in spontaneous magnetization, and can be switched by a magnetic field. This broad definition encompasses ferrimagnets (magnetite) and weak ferromagnets (hematite), as well as ordinary ferromagnets (iron). It does not include antiferromagnetic, paramagnetic and diamagnetic substances which have no spontaneous magnetization. Such materials are not ferromagnetic but may be ferrobimagnetic.

Magnetite is the best example of a magnetic mineral. Below 585°C , Fe_3O_4 is ferrimagnetic with a magnetic moment of 4 Bohr magnetons per molecule corresponding to the four unpaired electron spins associated with Fe^{2+} [2]. Tetrahedral Fe^{3+} spins are directed antiparallel to octahedral Fe^{3+} and Fe^{2+} spins so that the Fe^{3+} moments cancel,

leaving a spontaneous magnetization equivalent to one Fe^{2+} moment per molecule. The direction of easy magnetization is $\langle 111 \rangle$, giving rise to eight orientation states for $M_{(s)}$. Magnetite belongs to magnetic point group $\bar{3}m$, one of the 21 pyromagnetic classes (BIRSS, 1964) [15], although the trigonal distortion is too small to be seen by X-ray diffraction. Magnetic domains are difficult to see because magnetite is opaque in visible light, even in thin section. The domains are probably similar to those in MgFe_2O_4 which has the same magnetic structure, but is transparent to red wavelengths. SHERWOOD et al. [16] observed snake-like domain patterns in a (111) thin-section of magnesium ferrite.

Domains in transparent ferromagnetic and ferrimagnetic crystals are visible in polarized light because of the Faraday effect, a nonreciprocal rotation of the plane of polarization. The angle of rotation Φ is given by $\Phi = \rho t \cos \Theta$, where t is the specimen thickness, ρ the rotation per unit thickness, and Θ the angle between the magnetization vector and the direction of propagation. Faraday rotation coefficients for ferrites are typically about $1000^\circ/\text{cm}$ [16].

Hematite, $\alpha\text{-Fe}_2\text{O}_3$, exhibits both antiferromagnetism and weak ferromagnetism. From 250°K to 950°K , the Fe^{3+} spins lie in the rhombohedral (111) plane and are nearly antiparallel, but with a small ferromagnetic component, also in (111) . Mineralogists generally assign hematite to trigonal class $\bar{3}m$, but the magnetic point symmetry is $2/m$ at room temperature. Antiferromagnetic crystals often exhibit weak (parasitic) ferromagnetism when the ferromagnetic component does not violate the symmetry elements of the antiferromagnetic spin array [15]. In hematite, weak spontaneous magnetization appears along the monoclinic two-fold axis, corresponding to one of the three diad axes in $\bar{3}m$. At 250°K , the spin direction changes to the rhombohedral axis $[111]$ and the weak ferromagnetic effect disappears. Below the spin-flop transition, the magnetic point group is $\bar{3}m$.

Magnetic domains in hematite have been observed using the Faraday effect [17]. The white, gray and black regions in Fig.42 correspond to domains with three different magnetic axes; magnetic fields of only 10 oersteds produce significant differences in the domain pattern. When cooled through the spin-flop transition at -120°C , the domains disappear, and then reappear in a different pattern on heating.

A crystal is *ferroelastic* if it has two or more orientation states differing in spontaneous strain, and can be transformed from one to another of these states by an external mechanical stress. Spontaneous strain is measured relative to the prototype structure. In the ferroelastic state the crystal symmetry is reduced to a subgroup of a higher symmetry class by a small distortion, typically on the order of parts per thousand, which is a measure of the spontaneous strain $\epsilon_{(s)}$. By analogy with the ferro-

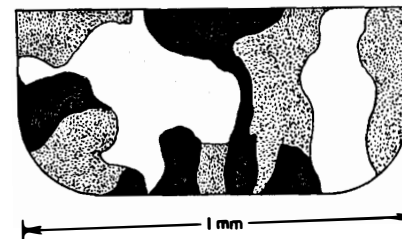


Fig. 42. Magnetic domain pattern in a hematite crystal observed by means of the Faraday effect. Three orientations of the parasitic ferromagnetism give rise to different light intensities. The specimen is a thin platelet ($\sim 0.03\text{ mm}$ thick) with major faces parallel to the rhombohedral (111) plane. To observe the domains it was necessary to tilt the platelet with respect to the light beam; otherwise the Faraday effect is absent because the magnetization vectors are perpendicular to the beam [17]

electric case, just as spontaneous polarization can be redirected by an electric field, the spontaneous strain of a ferroelastic can be reoriented by mechanical stress.

Ferroelasticity differs from ferroelectricity and ferromagnetism in one respect. Defining the zero reference for spontaneous strain is more subtle than that for spontaneous polarization or for spontaneous magnetization. If, in the absence of external forces, there is no electric or magnetic charge separation, then $P_{(s)} = M_{(s)} = 0$. To define $\epsilon_{(s)}$, a reference state of zero strain is required. The spontaneous strain of various orientation states may differ in sign or direction, but must be equal in magnitude, otherwise equivalent free energies are not obtained for equivalent stresses. When measured relative to the prototype structure, the $\epsilon_{(s)}$ values of all orientation states are equal in magnitude. Therefore, the prototype state containing all the pseudosymmetry elements is the zero reference for spontaneous strain.

Ferroelasticity is a type of mechanical twinning in which the lattice reorients rapidly in response to a mechanical stress. There is no diffusion or breaking of chemical bonds, only small rearrangements with atomic displacements of the order of 0.1 \AA . ABRAHAMS [18] has discussed the structural basis of ferroelasticity, emphasizing the importance of pseudosymmetry and citing a number of examples. The symmetry classification of potential ferroelastic materials has been developed by AIZU [11].

A summary of the earlier literature on mechanical twinning can be found in the book by KLASSEN-NEKLYUDOVA [19]. The book is divided into two parts: twinning with change in form, and twinning without

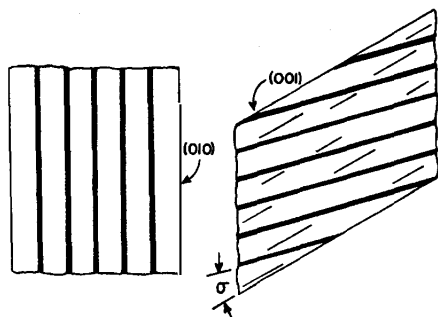


Fig. 43. Plagioclase feldspars exhibit perfect cleavage parallel to (001), and less perfect parallel to (010). Albite twin lamellae are usually present on (001) cleavage flakes (left). Albite lamellae are parallel to the straight edge formed by the intersection (010) and (001) cleavage planes. Flakes parallel to (010) sometimes show periclinic twins (right). Twin lamellae intersect the (001:010) edge at an angle σ , the so-called angle of the rhombic section. (After ROGERS and KERR [20])

change in form. Ferroelastic twinning is accompanied by a change in form associated with the reorientation of spontaneous strain. The triclinic feldspars show ferroelastic mechanical twinning. Twinning without change in form is exemplified by α -quartz. As discussed later, quartz is a ferrobielastic material with no spontaneous strain, but with orientation states which differ in elastic compliance.

Two views of the twin structure in triclinic feldspars are shown in Fig. 43. Twinning is common in all the feldspars, and almost universal in microcline (KAlSi_3O_8) and the plagioclases ($\text{NaAlSi}_3\text{O}_8$ – $\text{CaAl}_2\text{Si}_2\text{O}_8$) series). The extinction angles in twinned crystals constitute one of the chief methods of identifying feldspars. The two most important types of twins in feldspars are albite and pericline polysynthetic twins. Albite twin lamellae are parallel to (010), and are related by reflection across (010). This is a symmetry element in the prototype point group $2/m$ found in sanidine, the high-temperature potash feldspar. Microcline, the low-temperature polymorph, belongs to the centric class $\bar{1}$, as do the plagioclase feldspars. In pericline twins, the individuals are related by rotation of 180° about $[010]$, the two-fold symmetry axis in the prototype point group. The pseudosymmetry in plagioclase feldspars is caused by crumpling of the aluminosilicate framework about the Na^+ and Ca^{2+} ions (Fig. 44).

Strain is a symmetric second-rank tensor with six components: three longitudinal strains ϵ_{11} , ϵ_{22} , ϵ_{33} , and three shear components ϵ_{23} , ϵ_{13} , ϵ_{12} . The two orientation states in plagioclase feldspars are related by reflection across $b = X_2$. Reflection reverses the sign of X_2 , leaving X_1

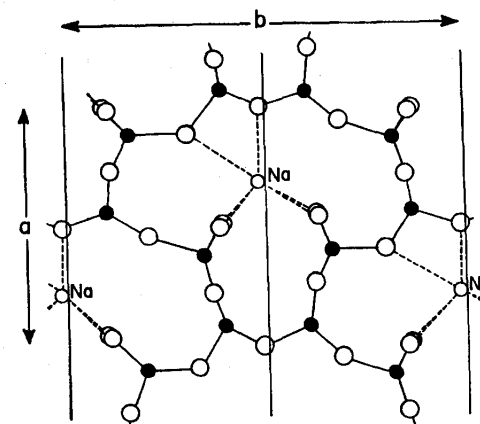


Fig. 44. Projection of the triclinic albite along the c -axis. The tetrahedral (Al, Si) ions (solid circles) and oxygens (open circles) form an aluminosilicate framework with Na^+ ions in cavities. Sodium ions are not large enough to contact all corners of the cavity so the framework is sheared and the symmetry is lowered from monoclinic to triclinic. Pseudo-mirror planes associated with the monoclinic prototype symmetry are shown as vertical dark lines [21]

and X_3 unchanged. Tensor components with an odd number of 2 subscripts change sign under this operation. Thus the non-zero components of spontaneous strain are $\epsilon_{(s)23}$ and $\epsilon_{(s)12}$, shearing strains about X_1 and X_3 , respectively.

The spontaneous strain associated with ferroelasticity in the plagioclase feldspars can be estimated from crystallographic data. For the varieties exhibiting mechanical twinning the cell angles are $\alpha = 93.5 \pm 0.5^\circ$, $\beta = 116.0 \pm 0.5^\circ$, $\gamma = 90.5 \pm 0.5^\circ$, compared to $\alpha = 90^\circ$, $\beta = 116.0 \pm 0.5^\circ$, $\gamma = 90^\circ$ for monoclinic feldspars. Adopting an orthogonal axial system $X_1 = a^*$, $X_2 = b$, $X_3 = c$, and neglecting the small difference between the triclinic γ and 90° , the two components of spontaneous strain are $\epsilon_{(s)12} = 0$ and $\epsilon_{(s)23} = (\pi/360^\circ)(\alpha - 90^\circ) = 0.03$. Compared to most ferroelastics, this is a rather large spontaneous strain. Based on this analysis, it appears that the difference in free energy for the two orientation states will take the form $\Delta G \cong 4\epsilon_{(s)23}\sigma_{23}$. The most effective stress in moving domain walls should be σ_{23} , a shearing stress about X_1 or a^* .

Mechanical twinning in anorthite was demonstrated by MÜGGE and HEIDE [22]. Albite and pericline twin lamellae spaced by about 0.03 mm were introduced under uniaxial stress. Coercive stresses were not measured, but are known to be considerably less than $25 \times 10^4 \text{ N/cm}^2$.

These observations were confirmed by LAVES [23]. Untwinned cleavage flakes of analbite ($\text{Na}_{0.8}\text{K}_{0.2}\text{AlSi}_3\text{O}_8$) were pressed lightly with the tip of a needle while viewed in a polarizing microscope. With changing pressure albite twin lamellae appear and disappear with changing widths.

Pressure-twinning is easier in high-temperature varieties, indicating the Al-Si ordering tends to "freeze-in" the twin states, raising the coercive stress. Ordered albite will not twin in response to pressure because strong chemical bonds have to be broken during twinning. The Si-Al distribution in albite has triclinic symmetry but in anorthite it is monoclinic. Therefore glide twinning is easier in ordered Ca-rich plagioclases. The relation between structural state and ease of formation of pericline-albite twins by gliding has been discussed by STARKEY [24].

11. Secondary Ferroics

Ferrobielectricity is a secondary ferroic phenomenon arising from field-induced electric polarization, rather than spontaneous polarization as in a ferroelectric. Switching between orientation states occurs because of differences in the dielectric permittivity tensor. Permittivity is a second-rank tensor like strain and magnetic susceptibility. Any orientation states differing in spontaneous strain will also differ in both electric and magnetic susceptibility. Therefore all ferroelastics are potentially ferrobielectric and ferrobimagnetic.

Ferrobielectricity can be expected in non-polar crystals with mimetic twinning and substantial dielectric anisotropy. Antiferroelectric materials such as NaNbO_3 and SrTiO_3 are promising candidates because the dielectric permittivities are large enough to make a sizeable contribution to the induced polarization term in the free energy function. Below 110 °K, SrTiO_3 is ferroelastic and possibly ferrobielectric. The phase transition involves a symmetry change from cubic (class $m\bar{3}m$) to tetragonal ($4/mmm$) at low temperatures. The TiO_6 octahedra of the ideal perovskite structure rotate about a four-fold axis. Alternate octahedra rotate clockwise and counterclockwise causing the structure to crumple about the Sr^{2+} ions [25]. On cooling through the transition the tetragonal c -axis may develop along any of the three cubic edges, giving rise to 90° domains. The domains are ferroelastic and optically-distinct. For stress-free 90° domains in SrTiO_3 , the difference in free energy will be proportional to $(\kappa_{33} - \kappa_{11}) E^2$. There is no apparent discontinuity in the dielectric constant or its slope at the cubic-tetragonal transition, but anisotropy in the permittivity develops at low temperatures. Dielectric

constants as large as 25000 have been reported [26]. Below 50 °K, electric double hysteresis loops are observed, along with changes in weak-field permittivity under DC bias. Such behavior may be associated with ferrobielectric domain wall movement.

Anisotropic magnetic susceptibility may lead to *ferrobimagnetism*. Magnetic susceptibility is a polar second-rank tensor like strain and electric permittivity, therefore ferrobimagnetism has the same symmetry requirements as ferroelasticity and ferrobielectricity. In materials with spontaneous magnetization, ferrobimagnetism will be masked by the larger ferromagnetic effect. The effect is most likely to occur in antiferromagnetic crystals since χ_{ij} is relatively small and isotropic in paramagnetic and diamagnetic solids.

Nickel oxide is both ferroelastic and ferrobimagnetic. At temperatures above the NÉEL point of 523 °K, NiO is paramagnetic with the cubic rocksalt structure. Below T_N , antiferromagnetic ordering of the Ni^{2+} spins results in a small rhombohedral distortion. The unit cell contracts slightly along one of the $\langle 111 \rangle$ body diagonals with the angle between cube axes changing from 90° to 90°4'. Crystallographic twinning occurs because the contraction may take place along any of the four body diagonals. Each domain is optically uniaxial with the optical axis parallel to the contraction direction. The birefringence ($n_e - n_o = 0.003$ at 5900 Å) is large enough to make domains visible in polarized light [27].

In a well-annealed crystal, domain walls are easily displaced by a mechanical stress (ferroelasticity) or by a magnetic field (ferrobimagnetism). Elastic energy is lowest for domains with the contraction axis parallel to the applied stress. The walls can be moved distances of several mm and the movement observed with a polarizing microscope. Only small mechanical stresses ($< 10 \text{ N/cm}^2$) are required to move domain walls. A multi-domain specimen can be converted to an untwinned state by pinching the crystal between thumb and index finger [28].

Untwinned NiO crystals possess an anisotropic magnetic susceptibility. For domains contracted along [111], the magnetic susceptibility parallel to [111] exceeds those measured in the perpendicular directions. At low fields the anisotropy in susceptibility is $3.3 \times 10^{-6} \text{ emu/g}$. In such a domain, spins lie in the (111) plane perpendicular to the [111] contraction direction. As in most antiferromagnetic materials, the magnetic susceptibility is largest perpendicular to the spins.

Moderate magnetic fields of 5000 oersteds are sufficient to move domain walls in well-annealed crystals. Induced magnetic energy (and total free energy) is minimized when the maximum magnetic susceptibility is parallel to the applied magnetic field. Antiferromagnetic domains with contraction direction parallel to H are favored over other orientations. The response to an applied field is highly erratic because the

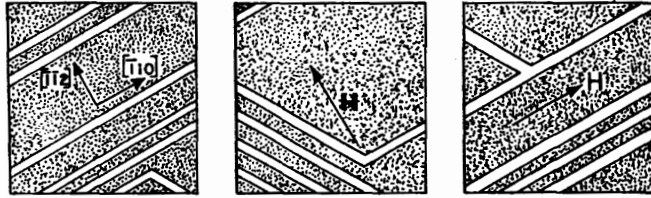


Fig. 45. Displacement of domain walls in antiferromagnetic NiO by a magnetic field. The crystal is a thin plate approximately 1 mm on edge with the major face parallel to (111). A magnetic field of 25000 oersteds was first applied along [112] and then along [110] to produce ferrobimagnetic switching. Domains are visible in polarized light because of the spontaneous strain associated with antiferromagnetic ordering. Viewed between crossed polarizer and analyzer, the major portion of the crystal is dark because the domains are contracted along [111]. Bright stripes sloping up to the left and up to the right correspond to domains contracted along [111] and [111], respectively [27]

walls are easily pinned by crystal imperfections. Domain wall movement in ferrobimagnetic NiO is illustrated in Fig. 45.

Ferrobielastic crystals are a class of secondary ferroics in which orientation states differ in elastic compliance, a fourth-rank polar tensor. Ferrobielastic switching in α -quartz has been reported by AIZU [10]. Under applied stress, the two twinned regions strain differently. This creates a difference in free energy favoring one domain over the other, causing domain walls to move. Ferrobielasticity is a second order effect in which the strain difference between orientation states is induced by applied stress. When the stress is removed, the induced strain and difference in free energy disappear also. Domain changes under stress can be observed optically because of differences in the photoelastic tensor for the two twin segments. Photoelasticity—the change in refractive indices with stress—is a fourth-rank tensor like elasticity. Orientation states differing in elastic constants will also differ in photoelastic coefficients.

β -quartz is hexagonal, crystal class 622. On cooling through the phase transition at 573° C, the symmetry is lowered to 32. Transformation twins develop as β -quartz converts to α -quartz. The transformation twins, often called Dauphiné twins or electrical twins, consist of two orientation states related by 180° rotation about [001], the trigonal axis. Dauphiné twins combine two right-handed (or two left-handed) individuals, often with irregular composition planes. Such twinning renders the crystals useless for piezoelectric applications because it reverses the direction of the X_1 axis and the signs of the piezoelectric coefficients. Because of the importance of piezoelectric quartz in communications

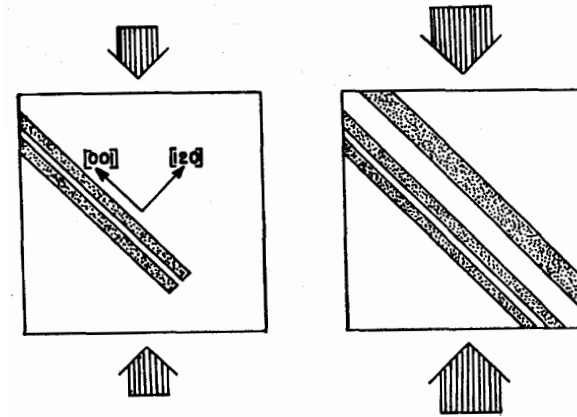


Fig. 46. Ferrobielastic switching of Dauphiné twins in quartz produced by uniaxial stress applied at 45° to X_2 and X_3 . As the mechanical stress is increased slowly from 4.9 to 5.0 newtons/cm², the striped twin pattern changes abruptly. Specimen dimensions are 5 × 5 × 3 mm. Orthogonal property axes (X_1, X_2, X_3) correspond to the [100], [120], [001] crystallographic axes, respectively. The crystal is viewed along X_1 between crossed polarizer and analyzer. Domains are visible because of the photoelastic effect; the contrast in brightness disappears when the stress is removed [11]

applications, techniques for detwinning quartz were developed during World War II when quartz was scarce. The mechanical detwinning of quartz demonstrated by THOMAS and WOOSTER [29] and by others [19], is an excellent example of ferrobielasticity.

When referred to the same axes, Dauphiné twin orientation states differ in elastic constants. Class 32 has six independent compliance coefficients: s_{1111} , s_{1122} , s_{1133} , s_{1123} , s_{3333} , and s_{2323} . The twins are related by 180° rotation about X_3 which reverses the signs of X_1 and X_2 . Polar tensor coefficients with an odd number of 1 and 2 subscripts change sign under such an operation. Therefore s_{1123} changes sign for the two orientation states but the other coefficients do not. Under an appropriate stress σ the difference in free energy between Dauphiné states is proportional to $s_{1123}\sigma^2$. As shown in Fig. 46, a uniaxial stress at 45° to X_2 and X_3 is effective in switching the ferrobielastic domains.

Atomic movements in the Dauphiné twin operation are small and do not involve the breaking of Si-O bonds. In shifting from one orientation state to the other, silicon atoms are displaced by 0.3 Å, and oxygens by about twice that amount. Across the composition plane there is a slight difference in bond angles. Dauphiné twinning disappears at the α - β transformation.

When referred to a common set of axes, the domain states of a true *ferroelastoelectric* differ in the piezoelectric tensor coefficients. The crystal can be switched from one state to another when an electric field and a mechanical stress are applied simultaneously. A ferroelastoelectric is not simply a ferroelectric which is also ferroelastic. Such materials can be switched by *either* an electric or mechanical force. *Both* forces are required to switch a true ferroelastoelectric, for it is neither ferroelectric nor ferroelastic.

Since all polar classes are potentially ferroelectric, a likely source of ferroelastoelectrics are the ten non-polar piezoelectric classes: 222, 32, $\bar{4}$, $\bar{4}2m$, 422, $\bar{6}$, $\bar{6}m2$, 622, 23, and $\bar{4}3m$. Quartz is a potential ferroelastoelectric since Dauphiné twins differ in piezoelectric constants as well as elastic constants.

Sal ammoniac (NH_4Cl) is the only proven ferroelastoelectric. Ammonium chloride undergoes a near second-order transition at -30°C accompanied by a λ -anomaly in the specific heat. The crystal structure is cubic, both above and below the transition, but the space group changes from $Pm\bar{3}m$ at room temperature to $P\bar{4}3m$ at low temperatures. The NH_4Cl structure resembles CsCl with N at $(0,0,0)$ and Cl at $(\frac{1}{2}, \frac{1}{2}, \frac{1}{2})$. Hydrogens lie along the body diagonals forming N-H-Cl hydrogen bonds. There are two possible orientations for the tetrahedral NH_4 group with hydrogens at $x, x, x; x, \bar{x}, \bar{x}; \bar{x}, x, \bar{x}; \bar{x}, \bar{x}, x$ ($x=0.153$), or at $\bar{x}, x, x; x, \bar{x}, x; x, x, \bar{x}; \bar{x}, \bar{x}, \bar{x}$. Neutron diffraction data recorded at room temperature favor Frenkel's model in which there is random disorder between the two orientations [30]. Measurements below the transition at liquid air temperature have established an ordered model with only one set of positions occupied [31].

In the absence of external forces the two orientation states are equal in energy, so that domains undoubtedly exist at low temperatures. Reflection across (100) brings the two states into coincidence. This is a very subtle type of twinning since the physical properties of the two orientation states are nearly identical. Only through third-rank tensor properties such as piezoelectricity and the electro-optic effect can the two states be distinguished.

Crystal class $\bar{4}3m$ has but one independent piezoelectric modulus d_{123} relating polarization along [100] to a shearing stress about [100]: $P_1 = d_{123}\sigma_{23}$. For the two orientation states, d_{123} is equal in magnitude but opposite in sign. Reflection across (100) takes X_1 to $-X_1$, and leaves X_2 and X_3 unchanged. Therefore d_{123} transforms to $-d_{123}$ for two domains related by a mirror parallel to (100).

Ammonium chloride is a potential ferroelastoelectric because its two orientation states differ in piezoelectric coefficients. Applying a uniaxial stress σ along [011] together with an electric field E along [100] leads

to a difference in free energy $G = 2d_{123}\sigma E$. Domain switching will take place if the driving potential ΔG is large enough to overcome the resistance to domain wall motion.

By influencing the domain structure of low temperature NH_4Cl , MOHLER and PITKA [32] were able to adjust the piezoelectric coefficient d_{123} from zero to a maximum value of $3 \times 10^{-12} \text{ m/V}$. Domain changes were induced by uniaxial stress ($\sim 10 \text{ bar}$) and a d.c. electric field ($\sim 10^6 \text{ V/m}$) applied simultaneously along [111] as the crystal was

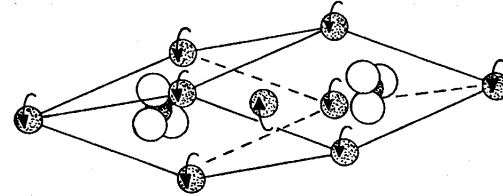


Fig. 47. Magnetic structure of siderite at low temperatures. Siderite has the calcite structure with Fe^{2+} ions at $(0,0,0)$ and $(\frac{1}{2}, \frac{1}{2}, \frac{1}{2})$ in the unit cell. The magnetic moment of the Fe atom at the origin is parallel to [111] and antiparallel to the moment at the cell center. Both spin directions are reserved in the other antiferromagnetic domain

cooled through the order-disorder transition. Earlier measurements [33] of the NH_4Cl piezoelectric coefficient were 100 times too small because domain contributions were not taken into account.

The domains of a *ferromagnetoelastic* material differ in piezomagnetic coefficients. Siderite (FeCO_3) is antiferromagnetic below 30°K . The magnetic structure (Fig. 47) consists of antiparallel Fe^{2+} spins aligned along the hexagonal c -axis [34]. Siderite belongs to crystal class $\bar{3}m$, and the magnetic point group is also $\bar{3}m$. Symmetry elements $\bar{3}'$ and m' , in which the spatial operation is accompanied by time-reversal, are absent. Crystals with magnetic symmetry $\bar{3}m$ are potentially piezomagnetic [15]. There are two independent piezomagnetic coefficients, Q_{222} and Q_{123} . Q_{222} relates a tensile stress along X_2 to a magnetization in the same direction; X_2 is the crystallographic [120] direction perpendicular to both the 2-fold (X_1) and 3-fold (X_3) symmetry axes. Piezomagnetic coefficient Q_{123} gives the magnetization component along X_1 resulting from a shearing stress about X_1 .

BOROVIK-ROMANOV et al. [35] have studied the piezomagnetic effect in iron carbonate crystals at liquid hydrogen temperature using a magnetic torsion balance in which a press containing the specimen is suspended between the pole pieces of the magnet. Q_{123} was measured, but Q_{222} was below the limit of observation. The magnitude of Q_{123} is

sensitive to bias during annealing. When cooled through the Néel point without stress bias, the effect was smaller, presumably because of antiferromagnetic domains. Domains in antiferromagnetic siderite are of the 180° type in which all spins are reversed (Fig. 47). The magnetic structures of neighboring domains are related by reflection across (2 $\bar{1}$ 0) accompanied by time reversal m' converting Q_{123} to $-Q_{123}$, so that the piezomagnetic coefficient is of opposite sign for the two domains. Siderite is therefore a potential ferromagnetoelastic crystal in which domains can be switched by applying mechanical stress and magnetic field simultaneously. The field should be directed along X_1 together with a shearing stress about X_1 .

The coupling between the electric and magnetic variables of a material is called the *magnetoelectric* effect. More specifically, it is a magnetization linearly proportional to an applied electric field. In analytic form the electrically-induced magnetoelectric effects is $M_i = \alpha_{ij} E_j$, and the magnetically induced effect is $P_i = \alpha_{ij} H_j$. The subscripts refer to the three directions of a right-handed Cartesian coordinate system and the α_{ij} coefficients are the field-independent magnetoelectric coefficients.

LANDAU and LIFSHITZ [36] employed symmetry arguments to predict the existence of the magnetoelectric effect and demonstrated that long-range magnetic order is a necessary, although not sufficient, requirement. Magnetoelectricity is permissible in 58 of the 90 magnetic point groups [15]. Recent advances in experimental techniques and theoretical understanding have been reviewed by BERTAUT and MERCIER [37]. Magnetoelectric coefficients have been measured for about twenty materials, including Cr_2O_3 , LiFePO_4 (triphylite) and LiMnPO_4 (lithiophilite).

LiFePO_4 undergoes a paramagnetic-antiferromagnetic phase transition at 50 °K. Magnetic susceptibility data collected in the paramagnetic region show typical Curie-Weiss behavior with an effective atomic moment of 5.45 μ_B and an extrapolated Curie constant of 88 °K [38]. BOZORTH and KRAMER [39] obtained comparable results on a mineral specimen of composition $\text{LiMn}_{0.7}\text{Fe}_{0.3}\text{PO}_4$: $T_N = 42$ °K, $\rho_{\text{eff}} = 6.1 \mu_B$, $\Theta = 80$ °K.

Triphylite is isostructural with olivine; lattice parameters for the orthorhombic unit cell are $a = 10.31$, $b = 6.00$, $c = 4.69$ Å. The space group is Pnma with four molecules per unit cell. Divalent iron atoms occupy mirror plane positions (equipoint 4c) with coordinates $\pm(0.28, 0.25, 0.98; 0.22, 0.75, 0.48)$. Low-temperature neutron diffraction studies gave a magnetic structure in which two of the Fe^{2+} spins are parallel to $+b$, the other two to $-b$. All four spins are reversed for the antiferromagnetic 180° domain.

The magnetic structure of triphylite conforms to magnetic point group mmm' , one of the magnetoelectric groups. The symbol m' means

that the mirror operation perpendicular to c includes a time reversal operator. Time reversal flips the spins by 180° since magnetic moments are associated with moving electric charge. The only non-zero magnetoelectric coefficients for mmm' are $\alpha_{12} = \alpha_{21}$. A value of 10^{-4} has been reported by BERTAUT and MERCIER [37]. In gaussian units, α is dimensionless.

Magnetoelectric measurements provide ample evidence for the existence of antiferromagnetic domains. The magnetoelectric coefficient α_{12} is identical in magnitude for the two domains but opposite in sign. If the sample is raised above the Néel temperature and cooled through the transition, the sign of α can be positive or negative. Rapid cooling produces both kinds of domains. Powder specimens exhibit no magnetoelectric effect unless annealed in bias fields to remove the degeneracy between the two domains [40]. The principle of the method is quite simple. In an electric field the induced magnetization for one domain is opposite to that of the other. If a magnetic field is then applied, the energies differ for the two time-reversed structures, making one more probable than the other. Poling works best just below the Néel point where coercive fields are smallest.

12. Ferroic Symmetry Species

The notation developed by AIZU [11] and SHUVALOV for ferroic species has found wide acceptance because it provides a compact description of the symmetry change accompanying a displacive phase transition. The cubic-tetragonal transition in BaTiO_3 at 120° C is represented by

$$m3m(3)D4F4mm.$$

The symbol begins with the high-temperature prototype point group ($m3m$) and ends with the low-temperature ferroic point group ($4mm$). F means the crystal is ferroelectric, and $D4$ indicates that the spontaneous polarization has definite orientation along the four-fold symmetry axis. There are three equivalent four-fold axes, denoted by (3) in the symbol. This is half the number of different domain orientations since the polarization can be directed along either the positive or negative directions.

The various ferroic species associated with a given prototype symmetry can be derived pictorially. Consider the tetragonal crystal class $\frac{4}{m} \frac{2}{m} \frac{2}{m} = 4/mmm$, the prototype symmetry of bismuth titanate ($\text{Bi}_4\text{Ti}_3\text{O}_{12}$). A polar vector representing spontaneous electric polari-

Table 12. Ferroelectric states for prototype symmetry $4/mmm$

Polarization direction	Components	
[001]	$P_x = P_y = 0 \neq P_z$	$4/mmm$ (1) D4 $F4mm$
[100]	$P_x \neq 0 = P_y = P_z$	$4/mmm$ (2) D2 $Fmm2$
[110]	$P_x = P_y \neq 0 = P_z$	$4/mmm$ (2) D2 $Fmm2$
[u0w]	$P_x \neq 0 = P_y \neq P_z$	$4/mmm$ (4) A2 Fm
[uuw]	$P_x = P_y \neq 0 \neq P_z$	$4/mmm$ (4) A2 Fm
[uv0]	$P_x \neq P_y \neq 0 = P_z$	$4/mmm$ (4) A4 Fm
[uvw]	$P_x \neq P_y \neq P_z \neq 0$	$4/mmm$ (8) A1 $F1$

zation is added to $4/mmm$ to derive the ferroelectric species; various derivative symmetries are possible depending on the orientation of the polarization vector. Placing the vector along z , the four-fold symmetry axis, destroys the mirror plane and the two-fold axes perpendicular to z . The symmetry of the ferroelectric state is therefore $4mm$, and the Aizu is $4/mmm$ (1) D4 $F4mm$. All seven ferroelectric species for prototype group $4/mmm$ are listed in Table 12. In the ferroelectric state $4/mmm$ (4) A4 Fm the polarization vector has an arbitrary direction in plane (001) perpendicular to the four-fold axis.

The symmetries of the ferroelectric states are polar subgroups of $4/mmm$, but not all polar subgroups of $4/mmm$ lead to ferroelectric states. Subgroups 2 and 4, for instance, are not found in Table 12.

Ferroelastic species are derived in a similar way. Spontaneous elastic strain is represented by a pair of equal but oppositely-directed vectors. Adding such a vector pair to the prototype symmetry generates the ferroelastic species. If the prototype symmetry is centric, the ferroelastic state will not be ferroelectric because the vector-pair will never destroy the center of symmetry. On the other hand, if the prototype symmetry is acentric, the spontaneous elastic strain may be accompanied by spontaneous polarization, making the state ferroelectric as well as ferroelastic. Piezoelectric coefficients couple strain to polarization. Adding a spontaneous strain along [110] to prototype symmetry $\bar{4}2m$ gives derivative symmetry $mm2$. Gadolinium molybdate is such a ferroelastic-ferroelectric.

A ferroelastic has two or more stable orientation states, even in the absence of applied forces, and can be transformed from one state to another by mechanical stress. As with ferroelectricity, pseudosymmetry exists on the microscopic scale with atom pairs located in nearly symmetric positions, differing by distances of 0.1 Å or less. Ferroelasticity is often accompanied by the onset of additional cooperative phenomena.

Gadolinium molybdate is a ferroelastic-ferroelectric, Nb_3Sn and V_3Si are ferroelastic-superconductors, and Mn_3O_4 is predicted to be a ferroelastic as well as ferrimagnetic [8].

Ferromagnetic species are somewhat more complicated because the magnetization vector is an axial tensor and the time reversal operator must be considered in deriving the magnetic point groups. Nevertheless, some interesting interaction phenomena arise because of magnetoelastic and magnetoelectric effects.

The symmetry requirements for primary ferroic materials have been examined by AIZU [11]. Of the 88 symmetry species for ferroelectrics, the spontaneous polarization can be reversed in direction for only 55. For the other 33, the P_s vector can be reoriented but not reversed. There are 94 fully ferroelastic species, of which $Pb_3P_2O_8$ is an example [41]. The Aizu symbol for lead phosphate is $\bar{3}m(3)D2F2/m$ indicating a symmetry change from trigonal point group $\bar{3}m$ to monoclinic point group $2/m$. Spontaneous strain develops along any of the three two-fold axes in $\bar{3}m$.

Although at present there are only a few well documented examples, secondary ferroic phenomena may prove to be rather common, since the symmetry requirements are not especially stringent [42]. Ferrobielectricity can be expected in any of the 94 ferroelastic species for crystals with substantial dielectric anisotropy. Strontium titanate belongs to species $m\bar{3}m(3)D4F4/m$. Nickel oxide and other antiferromagnetic ferroelastics can be expected to show ferrobimagnetism. Of the ninety magnetic point groups, 35 are potentially ferromagnetoelastic and 40 potentially ferromagnetoelastic. Ferrobielectric and ferroelastoelectric phenomena are somewhat less common since there only five pure ferrobielectric species and 15 pure ferroelastoelectrics, of which NH_4Cl is an example of species $m\bar{3}m(2)F\bar{4}3m$. Quartz is representative of species $622(2)F32$, one of the ten species which are both ferroelastoelectric and ferrobielectric.

References for Chapter IV

1. VON HIPPEL, A.R.: Dielectrics and waves. New York: John Wiley and Sons 1954.
2. SMITH, C.S.: In: SEITZ, F., TURNBULL, D. (Eds.): Solid state physics, Vol. 6, p. 175. New York: Academic Press 1958.
3. BEERMAN, H.P.: Bull. Am. Ceram. Soc. **46**, 737 (1967).
4. JAFFE, H.: Phys. Rev. **66**, 357 (1944).
5. TANENBAUM, M.: In: VON HIPPEL, A.R. (Ed.): The molecular designing of materials and devices, p. 227. Cambridge, Mass.: M.I.T. Press 1965.
6. NEWNHAM, R.E., WOLFE, R.W., DORRIAN, J.F.: Mat. Res. Bull. **6**, 1029 (1971).
7. NAKAMURA, E., MITSUI, T., FURUICHI, J.: J. Phys. Soc. Japan **18**, 1477 (1963).

8. ABRAHAMS, S.C., KEVE, E.T.: *Ferroelectrics* **2**, 129 (1971).
9. KEVE, E.T., BYE, K.L., WHIPPS, P.W., ANNIS, A.D.: *Ferroelectrics* **3**, 39 (1971).
10. AIZU, K.: *J. Phys. Soc. Japan* **34**, 121 (1973).
11. AIZU, K.: *Phys. Rev. B2*, 754 (1970).
12. GOLDSMITH, G.J.: *Bull. Am. Phys. Soc.* **1**, 322 (1956).
13. WEIDER, H.H.: *J. Appl. Phys.* **30**, 1010 (1959).
14. HAINSWORTH, F.N., PETCH, H.E.: *Can. J. Phys.* **44**, 3083 (1966).
15. BIRSS, R.R.: *Symmetry and magnetism*. Amsterdam: North Holland Publishing Co. 1964.
16. SHERWOOD, R.C., REMEIK, J.P., WILLIAMS, H.J.: *J. Appl. Phys.* **30**, 217 (1959).
17. WILLIAMS, H.J., SHERWOOD, R.C., REMEIK, J.P.: *J. Appl. Phys.* **29**, 1772 (1958).
18. ABRAHAMS, S.C.: *Mat. Res. Bull.* **6**, 881 (1971).
19. KLASSEN-NEKLYUDOVA, M.A.: *Mechanical twinning of crystals*. New York: Consultants Bureau 1964.
20. ROGERS, A.F., KERR, P.K.: *Optical mineralogy*. New York: McGraw-Hill Book Co. 1942.
21. BRAGG, W.L.: *Atomic structure of minerals*. Ithaca, N.Y.: Cornell University Press 1937.
22. MÜGGE, O., HEIDE, F.: *Neues j.b. Mineral. Abt. A64*, 163 (1931).
23. LAVES, F.: *Naturwissenschaften* **39**, 546 (1952).
24. STARKEY, J.: *Schweiz. Mineral. Petrogr. Mitt.* **47**, 257 (1967).
25. AXE, J.D.: *Trans. Am. Cryst. Assoc.* **7**, 89 (1971).
26. SAIFI, M.A., CROSS, L.E.: *Phys. Rev. B2*, 677 (1970).
27. ROTH, W.L.: *J. Appl. Phys.* **31**, 2000 (1960).
28. SLACK, G.A.: *J. Appl. Phys.* **31**, 1571 (1960).
29. THOMAS, L.A., WOOSTER, W.A.: *Proc. Roy. Soc. (Lond.) A* **208**, 43 (1951).
30. LEVY, H.A., PETERSON, S.W.: *Phys. Rev.* **86**, 766 (1952).
31. GOLDSCHMIDT, G.H., HURST, D.G.: *Phys. Rev.* **83**, 88 (1951).
32. MOHLER, E., PITKA, R.: *Solid State Commun.* **14**, 791 (1974).
33. BAHR, S., ENGL, J.: *Z. Phys.* **105**, 470 (1937).
34. PICKART, S.J.: *Bull. Am. Phys. Soc.* **5**, 357 (1960).
35. BOROVIK-ROMANOV, A.S., ALEKSANJAN, G.G., RUDASHEVSKII, E.G.: *Int. Conf. on Magnetism and Crystallography*. Kyoto, Japan, Paper 155, 1962.
36. LANDAU, L.D., LIFSHITZ, E.M.: *Electrodynamics of continuous media*. Reading, Mass.: Addison-Wesley Publishing Co. 1960.
37. BERTAUT, E.F., MERCIER, M.: *Mat. Res. Bull.* **6**, 907 (1971).
38. SANTORO, R.P., NEWNHAM, R.E.: *Acta Cryst.* **22**, 344 (1967).
39. BOZORTH, R.M., KRAMER, V.: *J. Phys. Radium* **20**, 393 (1959).
40. SHTRIKMAN, S., TREVES, D.: *Phys. Rev.* **130**, 986 (1963).
41. BRIKNER, L.H., BIERSTEDT, P.E., JAEP, W.F., BARKLEY, J.R.: *Mat. Res. Bull.* **8**, 497 (1973).
42. NEWNHAM, R.E., CROSS, L.E.: *Mat. Res. Bull.* **9**, 927, 1021 (1974).

V. Optical Materials

The refractive index for transparent materials is equal to the ratio of the speed of light in vacuum to that in the material. Because of their low densities, gases have refractive indices near 1, while for liquids and solids n ranges between 1.3 and 3. The magnitude of n is determined chiefly by density of packing and the polarizability of the ions. Densely packed arrays of highly polarizable groups result in large refractive indices.

Refractive index depends on wavelength, giving rise to dispersion. For most transparent substances, n increases as λ decreases; refractive indices for violet light are generally a few percent larger than those for red. Dispersion is caused by electronic transitions in the ultraviolet region. When the photon energy approaches the value required for transition, the electrons undergo wide excursions, producing large polarizability and large refractive indices.

Many of the new devices proposed for optical communication systems require transparent materials with large refractive indices. This means that materials with transitions in the near ultraviolet are of special interest. The index of refraction is inversely related to the band gap E_g . WEMPLE and DIDOMENICO [1] have shown that for oxides the relation approximates

$$n^2 \cong 1 + \frac{15}{E_g},$$

where E_g is expressed in electron-volts. Other classes of materials may have somewhat different constants. If an oxide is to be transparent throughout the visible range, the equation states that the band gap must be at least $hc/4000 \text{ Å} \cong 3 \text{ eV}$, giving $n \cong 2.5$. To obtain higher refractive indices, the minimum wavelength must be raised, closing the window. The shortest wavelength for which transmission is desired determines the maximum refractive index.

The empirical Gladstone-Dale relation is useful in predicting refractive indices,

$$n = 1 + \rho \sum_i p_i k_i,$$

where ρ is density, and p_i and k_i are the weight fraction and refractive coefficient of the i th component. An abbreviated table of refractive co-